Int. J. Electrochem. Sci., 16 **(2021)** Article ID: 210761, doi: 10.20964/2021.07.60

International Journal of
ELECTROCHEMICAL
SCIENCE
www.electrochemsci.org

Sensitive Electrochemical Detection of Caffeic Acid using a Carboxyl-Functionalized Reduced Graphene Oxide-Modified Glassy Carbon Electrode (ERGO-COOH/GCE)

Ming Zhou, Yong Xu, Rong Zhong, Yurong Wang[*]

School of Pharmaceutical Sciences, Zhejiang Chinese Medical University, Hangzhou 310053, China
[*]E-mail: wangyr@zcmu.edu.cn

Received: 17 March 2021 / *Accepted:* 29 April 2021 / *Published:* 31 May 2021

A glassy carbon electrode modified by carboxyl-functionalized reduced graphene oxide (ERGO-COOH/GCE) was developed by electrochemical deposition method. The electrochemical behavior of caffeic acid (CA) on the ERGO-COOH/GCE was studied, and an electroanalytical method for the detection of CA in tablets was established. The effects of the modification parameters, the pH of the buffer solution and the scanning rate on the electrochemical behavior of CA were investigated by cyclic voltammetry (CV). The results revealed that modifying the GCE by electrochemical deposition facilitated a more sensitive response to CA on the modified electrode than modifying it by drop coating. The peak current of CA on the ERGO-COOH/GCE was significantly higher than that on the bare glassy carbon electrode (GCE) over five scan cycles, and the optimized the concentration of GO-COOH, the scanning cycles, and the pH were 4 mg·mL^{-1}, 5 cycles, and 2.0, respectively. The redox reaction of CA on the modified electrode was a quasi-reversible process controlled by adsorption and involved the transfer of two electrons and two protons. The ERGO-COOH/GCE showed a linear response to CA in the range of 0.05 ~ 20 μM with a limit of detection of 8 nM (*S/N*=3). The modified electrode exhibited good repeatability and reproducibility and anti-interference performance. The ERGO-COOH/GCE was applied to the detection of CA in caffeic acid tablets with a recovery of 97.7% ~ 108%.

Keywords: Caffeic acid; electrochemical deposition; ERGO-COOH/GCE; modified electrode; differential pulse voltammetry

1. INTRODUCTION

Caffeic acid (CA, 3,4-dihydroxycinnamic acid) with the molecular formula of $C_9H_8O_4$ is a kind of phenolic compound (Fig. 1) that often exists in Chinese medicinal herbs such as Solidago, thymus, Cimicifuga, Eucommia ulmoides, etc. CA has multiple pharmacological activities, including anti-inflammatory and antiviral activity and increased white blood cell and platelet counts. Therefore, it is mostly used in the prevention and treatment of diseases related to oxidative stress, inflammatory

reactions, and viral infections, such as brain tissue damage [6], cardiovascular disease [7], human immunodeficiency virus (HIV) infection [8], leukopenia and thrombocytopenia [9]. Due to its important pharmacological activities, it is necessary to develop a simple, rapid, and low-cost analytical method for the determination of CA content.

In recent years, various analytical methods have been developed to analyze the content of CA, including high-performance liquid chromatography [10], capillary electrophoresis [11], liquid mass spectrometry/mass spectrometry [12], and electrochemical methods [13]. By comparison, electrochemical methods have been widely used in the analysis and determination of many electroactive drugs [14-16] because of their low technical cost, sensitivity and rapid analysis, easy miniaturization, and easy operation. CA has a phenolic hydroxyl group, carboxyl group, and other electroactive groups that can undergo redox reactions within a certain potential range. Thus, several modified electrodes have been prepared and reported for the detection of CA. Karikalan [17] et al. prepared a nitrogen-doped carbon-modified electrode (NDC/GCE) for electrochemical determination of CA in red wine with a linear range of 0.01~350 μM, and a detection limit of 4 nM (*S/N* = 3). Manikandan [18] et al. prepared a fluorine-doped graphene oxide modified electrode (F-GO/GCE) for electrochemical determination of CA in red wine with a linear range of 0.5~100 μM and a detection limit of 18 nM (*S/N* = 3). Gao [19] et al. prepared a Pt-PEDOT/reduced graphene oxide modified electrode (F-GO/GCE) for electrochemical determination of CA in green tea and black tea with a linear range of 0.005~50 μM and a detection limit of 2 nM (*S/N* = 3). These reports reveal that electrochemical methods have great potential in the qualitative and quantitative determination of CA in food texture. However, the determination of CA in drugs has not been as successful and most studies have reported problems of complex preparation methods, narrow linear ranges, and high detection limits. Tyszczuk [20] et al. prepared a lead film modified electrode (PdFE/GCE) for electrochemical determination of CA in Plantago lanceolata with a linear range of 0.08~0.5 μM, and a detection limit of 0.4 nM (*S/N* = 3).

With the rapid development of nanotechnology, graphene and graphene oxide (GO) have been the focus of attention due to their large theoretical specific surface area, high theoretical capacitance, and good thermal conductivity [21-23]. Carboxylated graphene oxide (GO-COOH) is a derivative of GO that shows a higher specific surface area, easier preservation, and better conductivity than GO. It can covalently combine with electrode materials and can be better dispersed in solution [24]. In recent years, an increasing number of scientists have used GO-COOH as an electrode-modified material for electrochemical detection. For example, Dilmac [25] et al. prepared a carboxylated graphene oxide Au nanocomposite-modified electrode (GO-COOAu/GCE) by the drop coating method for electrochemical determination of glucose in human serum samples with a linear range of 0.02~4.48 μM and a detection limit of 6 μM (*S/N* = 3). Song [26] et al. prepared a carboxylated graphene oxide polyethyleneimine nanocomposite-modified electrode (GO-COOH/PEI/GCE) by the drop coating method for electrochemical determination of sensing with a linear range of 27~120 μM and a detection limit of 950 nM (*S/N* = 3). To data, there have been no reports of GO-COOH modified on an electrode by electrodeposition to detect CA.

In this paper, a glassy carbon electrode was modified with carboxyl functionalized reduced graphene oxide (ERGO-COOH/GCE) by electrochemical deposition [27] for the detection of CA. Compared with the reported methods, the modified electrode had the advantages of simple preparation,

good reproducibility, and better detection performance. Furthermore, the real sample analysis of CA in caffeic acid tablets showed the practicability of this electrode.

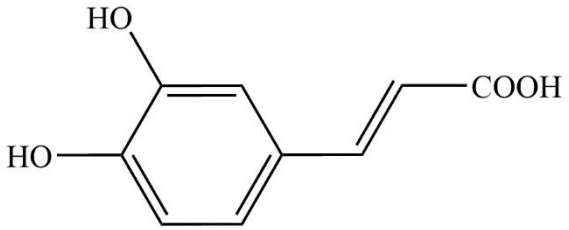

Figure 1. The chemical structure of CA

2. EXPERIMENTAL

2.1. Reagents and instruments

Carboxylated graphene oxide (GO-COOH) was purchased from Nanjing Xianfeng nano Co., caffeic acid (HPLC≥99%) was purchased from Aladdin Chemistry Co., caffeic tablets were provided by Dezhou Deyao Pharmaceutical Co. The supporting electrolyte for electrochemical detection was 0.04 M Britton-Robinson buffer solution (B-R, pH = 2.0). All the other chemicals were of analytical grade or better. Ultrapure water (electrical resistance of 18.2 MΩ·cm) obtained from a Smart-DUVF water purification system (Shanghai Hitech Instruments Co., Ltd., China) was used to prepare all solutions.

A CHI660 electrochemical workstation (Shanghai Chenhua Instrument Co. Ltd., Shanghai, China) was used to perform cyclic voltammetry (CV) and differential pulse voltammetry (DPV). An RST5210F electrochemical workstation (Suzhou Risetest Electronic Co., Ltd., Suzhou, China) was used to perform electrochemical impedance spectroscopy (EIS). A conventional three-electrode system was used for electrochemical detection with an ERGO-COOH/GCE as the working electrode and Ag/AgCl and a Pt wire as the reference electrode and counter electrode, respectively.

2.2. Preparation of the ERGO-COOH/GCE

Before modification, the bare GCE was successively polished with 0.3, 0.1, and 0.05 μm alumina slurries. Then, the electrodes were sonically washed in ethanol and ultrapure water for 3 min each. Finally, the samples were dried in air at room temperature.

GO-COOH was ultrasonically dispersed in a PBS solution (pH = 5.75) for 2 h to obtain a homogenous dispersion (4 mg·mL^{-1}). Next, the polished GCE was immersed in the GO-COOH modified solution for CV ranging from 0.6 V to -1.5 V at a scan rate of 0.025 V·s^{-1} for 10 cycles for electrochemical deposition of GO-COOH on the surface of the GCE to obtain the ERGO-COOH/GCE. The obtained electrode was washed with ultrapure water and dried at room temperature.

2.3. Real sample solution preparation

The tablet powder was obtained from 10 caffeic acid tablets (0.1392 g·tablet^{-1}) finely powdered in an agate mortar. An accurate weight of 0.1252 g powder (approximately 80 mg CA) was transferred into a 100 ml volumetric flask, and 40 ml ethanol, 2 ml hydrochloric acid solution (0.1 M) were added, the flask was filled to the scale line with ultrapure water. After shaking well, the sample solution was obtained by centrifugation and filtration. Before each measurement, the desired concentration of sample was prepared with the supporting electrolyte.

3. RESULTS AND DISCUSSION

3.1. Optimization of modification conditions

3.1.1. Influence of modification methods

While drop coating was mostly used to modify GO-COOH on the electrode surface in prior studies [28,29], electrodeposition was applied in this work to modify the bare GCE surface with GO-COOH. The electrochemical performances of the electrodes prepared by drop coating and electrodeposition were compared by EIS and the detection of CA.

EIS was performed on the bare GCE, GO-COOH/GCE, and ERGO-COOH/GCE in 5 mM $K_3[Fe(CN)_6]/K_4[Fe(CN)_6]$ solution (containing 0.1 M KCl), and the results are shown in Fig. 2A. The Nyquist impedance spectrum consists of a semicircle and a straight line, and the diameter of the semicircle in the high frequency region corresponds to the electron transfer impedance (Ret) [30]. Fig. 2A shows that the semicircle diameter of ERGO-COOH/GCE is significantly smaller than that of GO-COOH/GCE and GCE. The Ret values of the bare GCE, GO-COOH/GCE, and ERGO-COOH/GCE were calculated to be approximately 149, 94, and 48 Ω, respectively. The results demonstrated that the electrodeposited ERGO-COOH film was beneficial for accelerating the electron transfer process and enhancing the conductivity of the electrode. The results further prove that ERGO-COOH is modified on the electrode surface.

To estimate the active area of electrodes, the redox properties of the GCE, GO-COOH/GCE, and ERGO-COOH/GCE were studied in a 1 mM $K_3[Fe(CN)_6]/K_4[Fe(CN)_6]$ solution containing 0.1 M KCl at different scan rates from 0.02 to 0.3 V·s^{-1}. The electrode active surface areas of the detected electrodes were calculated by the Randles-Sevcik equation (1) [31],

$$I_p = 2.69\times10^5 \cdot n^{3/2} \cdot C \cdot D^{1/2} \cdot A \cdot v^{1/2} \quad (1)$$

where I_p (A) is the redox peak current, n is the number of electrons transferred, C (M) is the concentration of the $K_3[Fe(CN)_6]/K_4[Fe(CN)_6]$ solution, D (cm^2·s^{-1}) is the diffusion coefficient, A (cm^2) is the active area of the working electrode, and v (V/s) is the scan rate. The results showed that the redox peak currents (I) of the GCE, GO-COOH/GCE, and ERGO-COOH/GCE had a good linear relationship with the square root of the scan rate ($v^{1/2}$), and the slopes of the linear equations were 36.98, 40.40,

111.74 $\mu A \cdot s^{1/2} \cdot V^{-1/2}$, respectively. By substituting the above slopes in equation (1), the active areas of the above electrodes were calculated to be 0.050, 0.055, and 0.151 cm^2. The effective area of the ERGO-COOH/GCE was 3.0 and 2.7 times that of the GCE and GO-COOH/GCE, respectively, which indicated that the modified layer of ERGO-COOH formed by electrodeposition has a larger effective area than the modified layer of GO-COOH formed by the drop coating method, which can improve the detection sensitivity.

Fig. 2B shows the CV plots of CA on the GCE, GO-COOH/GCE, and ERGO-COOH/GCE. The redox peak current of CA on ERGO-COOH/GCE prepared by electrodeposition is significantly higher than that on the GO-COOH/GCE prepared by the dropping coating method. This is because the graphene oxide was reduced to reduced graphene oxide, and reduced graphene oxide has higher conductivity [32] and a larger electrochemical active area than graphene oxide. Therefore, we chose the ERGO-COOH/GCE prepared by the electrodeposition method to further establish the method for CA detection.

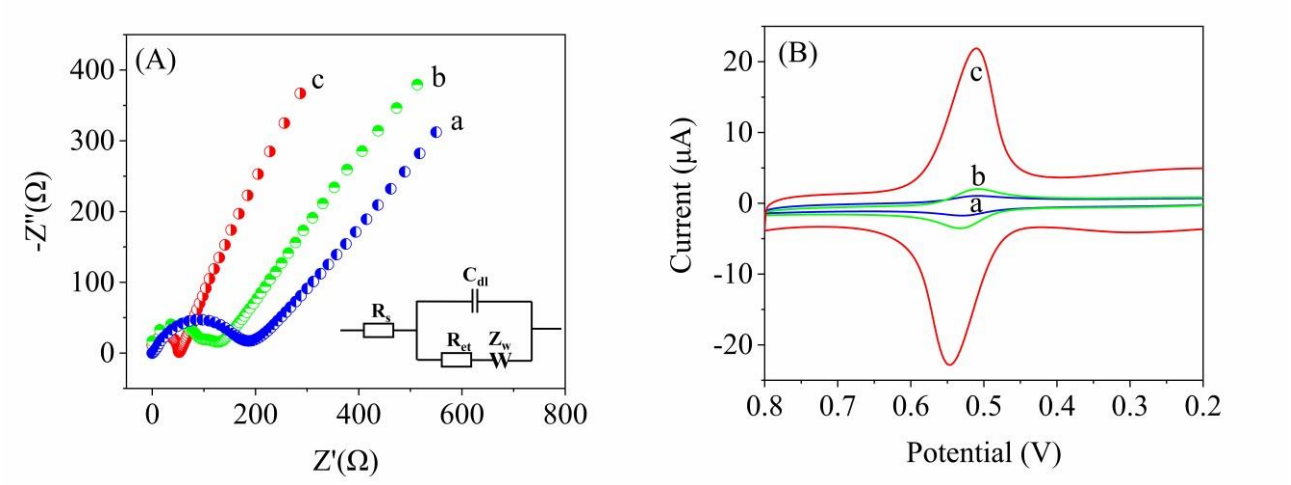

Figure 2. (A) EIS of the GCE (a), GO-COOH/GCE (b), and ERGO-COOH/GCE (c) in 5 mM $K_3[Fe(CN)_6]/K_4[Fe(CN)_6]$ solution containing 0.1 M KCl. (B) CV curves of 5 μM CA on the GCE (a), GO-COOH/GCE (b), and ERGO-COOH/GCE (c) in 0.04 M B-R buffer solution (pH = 2.0) at a scan rate of 0.05 $V \cdot s^{-1}$.

3.1.2. Effect of the modified solution concentration

Fig. 3 shows the effect of the amount of GO-COOH on the response of CA on the ERGO-COOH/GCE. The redox peak current of CA gradually increased with increasing concentration of the GO-COOH modification solution. When the GO-COOH solution concentration was 4 $mg \cdot mL^{-1}$, the current reached the maximum and tended to be stable. Therefore, 4 $mg \cdot mL^{-1}$ was selected as the optimal concentration of the modification solution.

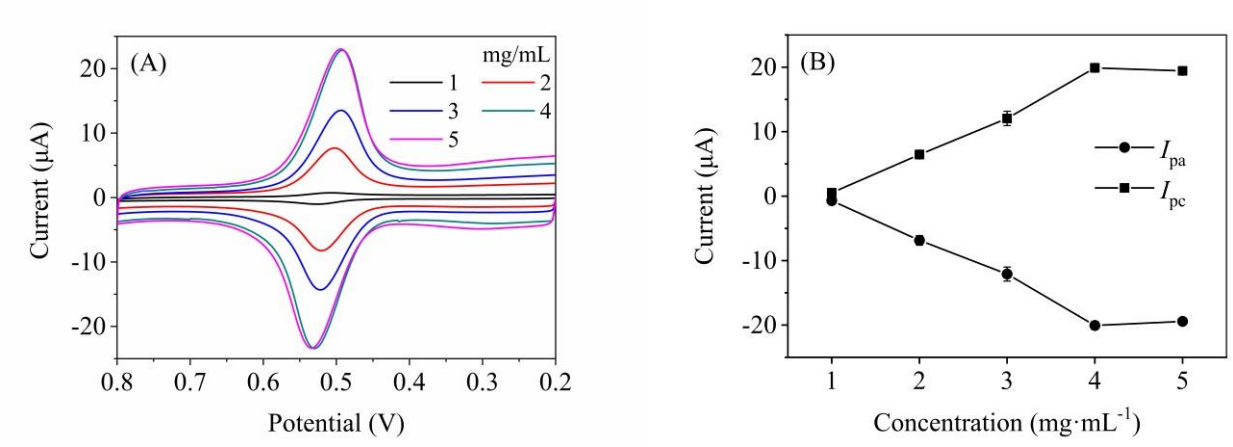

Figure 3. Effect of GO-COOH concentration (1, 2, 3, 4, 5 mg·mL^{-1}). (A) CV curves of CA on ERGO-COOH/GCE modified with different concentrations of GO-COOH in 0.04 M B-R buffer solution (pH = 2.0) at a scan rate of 0.05 V·s^{-1}. (B) The relationship between the redox peak current and the concentration of GO-COOH.

3.1.3. Effect of the scanning cycle

The scanning cycle determines the thickness of the surface of the modified electrode and affects CA detection. Thus, the effect of ERGO-COOH/GCE with different CV scanning cycles on the detection of CA was investigated. As shown in Fig. 4, the scanning cycles increased from 0 to 5, the coverage rate of ERGO-COOH on the electrode surface increased, and the effective surface area detected by the electrode increased, resulting in a significant increase in the peak current. When the scanning cycles exceeded 5, the peak current decreased, which was due to the saturation of ERGO-COOH on the electrode surface and the increase in thickness, which hindered the electronic exchange between CA and electrode [33]. Therefore, we chose 5 as the number of scanning cycles for electrodeposition.

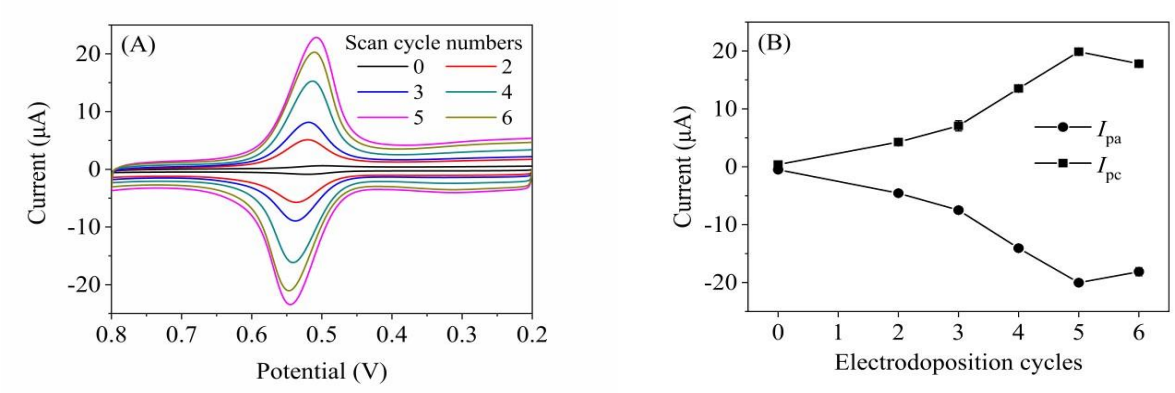

Figure 4. The effect of different numbers of electrodeposition cycles (0, 2, 3, 4, 5, 6). (A) CV curves of CA on ERGO-COOH/GCE modified with different electrodeposition cycles in 0.04 M B-R buffer solution (pH = 2.0) at a scan rate of 0.05 V·s^{-1}. (B) The relationship between the redox peak current and the electrodeposition cycle.

3.2. Electrochemical behavior of CA at the ERGO-COOH/GCE

3.2.1. Effect of pH

The effect of the pH of the supporting electrolyte on the response of CA on the ERGO-COOH/GCE was investigated by CV in B-R over a pH range of 2.0 ~ 4.5. As shown in Fig. 5, when the pH was 2.0, the oxidation peak current of CA reached its maximum value, and the redox peak decreased as the pH continually increased. This response might be due to the absence of protons in CA when the pH increased gradually, which made it difficult for the phenolic hydroxyl group in CA to undergo electrochemical reactions. It can also be seen from Fig. 5 that the redox peak potential moved to the negative potential direction with increasing pH, indicating that protons participated in the electrode reaction. The oxidation peak potential (E_{pa}) and the reduction peak potential (E_{pc}) have good linear relationships with pH. The linear regression equations can be expressed as E_{pa} (V) = – 0.0575 pH + 0.6692 (R^2 = 0.9863) and E_{pc} (V) = – 0.0593 pH + 0.6254 (R^2 = 0.9959). The linear slopes of the oxidation peak and the reduction peak are –59.3 mV·pH^{-1} and –57.5 mV·pH^{-1}, respectively, which are close to the theoretical value of –59.2 mV·pH^{-1}, indicating that protons participate in the electrochemical reaction of CA, and the number of protons is equal to that of the transferred electrons [34]. In the following experiments, a pH of 2.0 was chosen for further experiments.

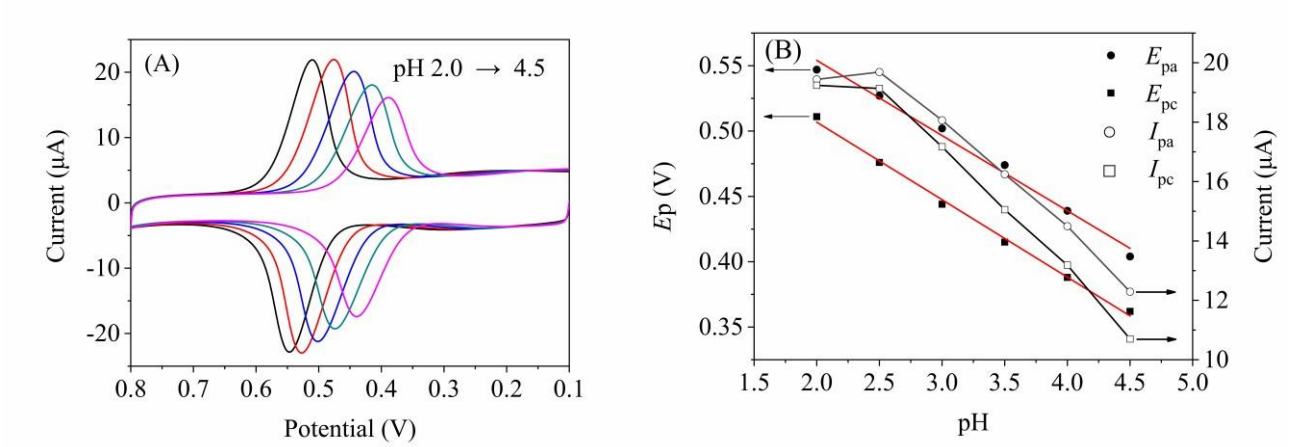

Figure 5. (A) CVs of CA (5 μM) on the ERGO-COOH/GCE in 0.04 M B-R at different pH (2.0, 2.5, 3.0, 3.5, 4.0, 4.5) and a scan rate of 0.05 V·s^{-1}. (B) pH-dependence of E_p and I.

3.2.2. Effect of the scan rate

The effect of the scan rate on the response of CA on ERGO-COOH/GCE was investigated by CV at different scan rates from 0.02 V·s^{-1} to 0.30 V·s^{-1}. As shown in Fig. 6A, the redox peak currents of CA increased continuously with increasing scan rate. Both the oxidation peak current (I_{pa}) and the reduction peak current (I_{pc}) have good linear relationships with the scan rate (v), and the linear regression equations can be expressed as I_{pa} (μA) = – 208.067 v (V·s^{-1}) – 5.553 (R^2 = 0.9921) and I_{pc} (μA) = – 205.780 v (V·s^{-1}) – 5.220 (R^2 = 0.9924), suggesting that the reaction of CA on the ERGO-COOH/GCE is an adsorption-controlled process [35]. As shown in Fig. 6A, an increase in the scan rate resulted in a

positive shift in the oxidation peak potential (E_{pa}), and a negative shift in the reduction peak potential (E_{pc}), indicating a quasi-reversible electrode process.

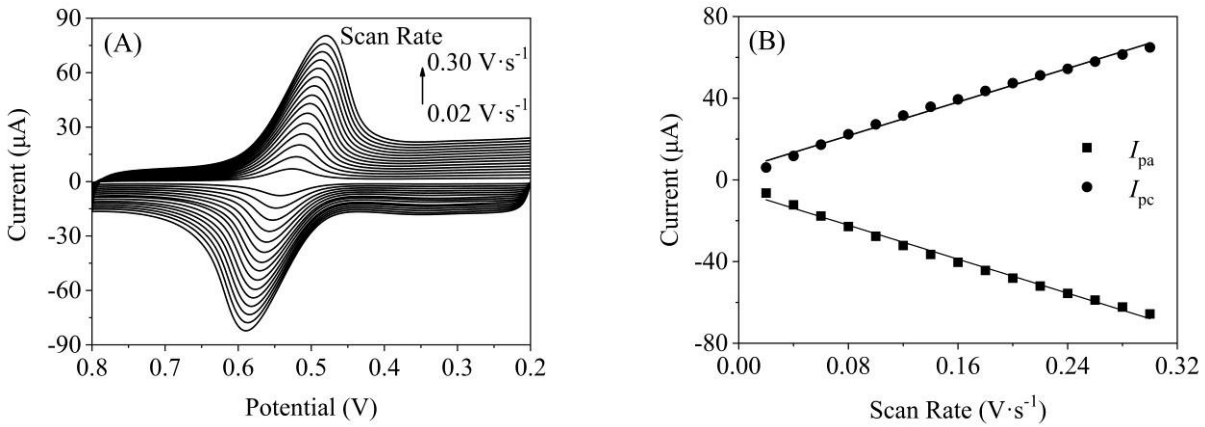

Figure 6. (A) CVs of CA (5 μM) on the ERGO-COOH/GCE in 0.04 M B-R (pH = 2.0) at different scan rates (0.02 V·s^{-1} to 0.30 V·s^{-1}) with 20 mV·s^{-1} intervals. (B) The linear relationship between the redox peak current and the scan rate.

Furthermore, when $v > 0.10$ V·s^{-1}, the plots between the redox peak potential (E) and the natural logarithm of scan rate (ln$v$) exhibited two good linear relationships with the regression equations of E_{pa} (V) = 0.02553ln$v$ + 0.6183 (R^2 = 0.9867) and E_{pc} (V) = –0.02562ln$v$ + 0.4517 (R^2 = 0.9836). For the model of a surface-controlled process, the electron transfer kinetics of CA on the ERGO-COOH/GCE could be deduced by the Laviron equations (2-4) [36],

$$E_{pa} = E^{0'} + \frac{RT}{(1-\alpha)nF}\ln v \quad (2)$$

$$E_{pc} = E^{0'} - \frac{RT}{\alpha nF}\ln v \quad (3)$$

$$\lg k_s = \alpha\lg(1-\alpha) + (1-\alpha)\lg\alpha - \lg\frac{RT}{nFv} - \alpha(1-\alpha)\frac{nF\Delta E_p}{2.303RT} \quad (4)$$

Note that $E^{0\prime}$ is the formal standard potential, k_s is the apparent heterogeneous electron transfer rate constant, n is the electron transfer number, α is the charge transfer coefficient, v is the scan rate, R is the gas constant, F is Faraday's constant, and ΔE_p is the peak-to-peak potential separation.

According to the slopes of E_{pa}-ln$v$ and E_{pc}-ln$v$, the values of α and n were calculated to be 1.9 and 0.50, respectively. Therefore, the number of electrons involved in the redox reaction of CA on ERGO-COOH/GCE was found to be 2. Additionally, k_s was calculated to be 1.5 s^{-1} according to equation (4).

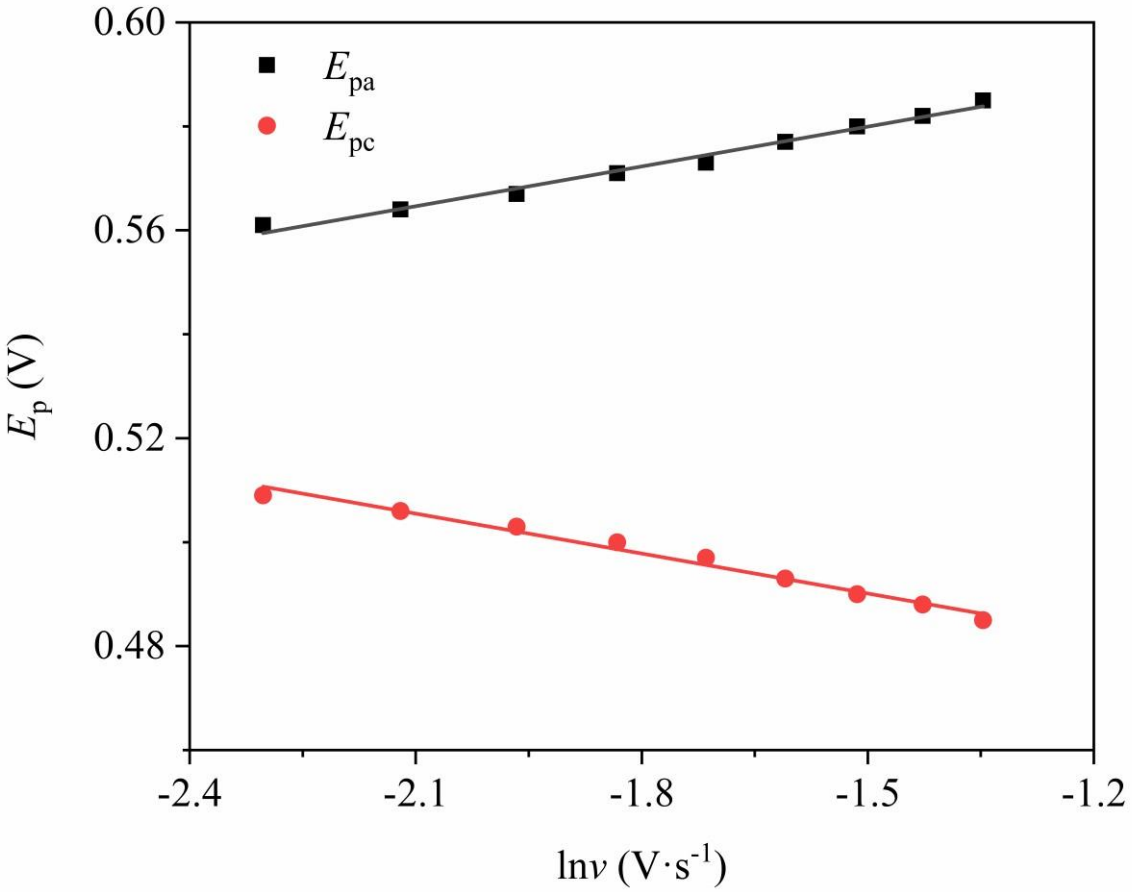

Figure 7. Relationship between the redox peak potential and ln$v$ deduced from Fig. 6A.

All the above results indicate the electrochemistry of CA on ERGO-COOH/GCE was a two-proton two-electron process. The reaction is shown in Fig. 8 and was consistent with the reported electrochemical detection of CA [20].

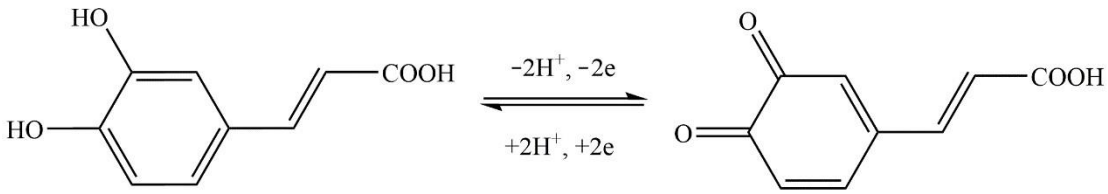

Figure 8. The electrochemical reaction of CA on the ERGO-COOH/GCE

3.2.3. Chronocoulometric studies

Because CA detection on the ERGO-COOH/GCE is an adsorption-controlled process, single potential step chronocoulometry can be used to calculate the Faraday charge (Q_{ads}), the diffusion

coefficient (D), and the saturated adsorption capacity (Γ^*) of CA on the ERGO-COOH/GCE surface. For this system, the potential was stepped from 0.1 to 0. 8 V, and the Q-t curves were performed in the absence (Fig. 9A, curve a) and presence (Fig. 9A, curve b) of CA (5 μM) in 0.04 M B-R (pH = 2.0). The corresponding Q-$t^{1/2}$ plots are shown in Fig. 9B.

The linear relationship of Q-$t^{1/2}$ corresponded to the following equations, Q (μC) = $-18.64t^{1/2} - 80.54$ (R^2 = 0.9998) and Q (μC) = $-22.71t^{1/2} - 204.72$ (R^2 = 0.9957) for the absence and presence of CA, respectively. In Anson equations (5) and (6) [37], Q_{dl} is the double-layer charge, Q_{ads} is the Faraday charge due to the oxidation of adsorbed CA, F is the Faraday constant, A (cm^2) is the active area of ERGO-COOH/GCE, c (mol·cm^{-3}) is the concentration of CA, n is the number of electrons transferred and D (cm^2·s^{-1}) is the diffusion coefficient.

$$Q = \frac{2nFAC(Dt)^{1/2}}{\pi^{1/2}} + Q_{dl} + Q_{ads} \quad (5)$$

The value of Q_{ads} was calculated to be 1.24 × 10^{-4} C, and D was 1.91 × 10^{-8} cm·s^{-1}. The Γ^* of CA on the ERGO-COOH/GCE was determined to be 4.26 ×10^{-9} mol·cm^{-2} according to equation (6)

$$Q_{ads} = nFA\Gamma^* \quad (6)$$

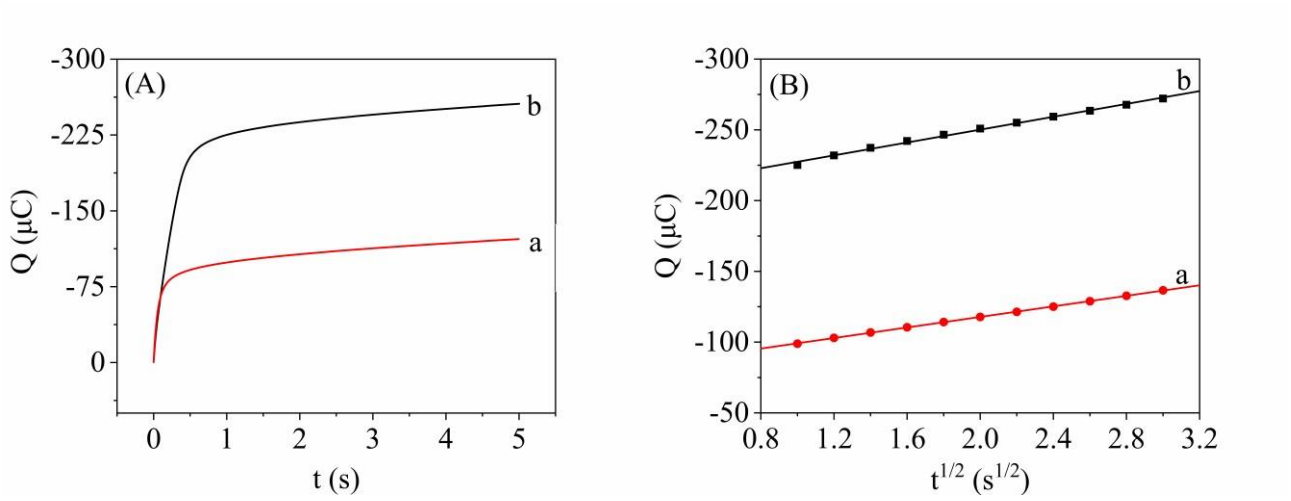

Figure 9. (A) Chronocoulometric curves in the absence (curve a) and presence (curve b) of 5 μM CA in 0.04 M B-R (pH 2.0) on ERGO-COOH/GCE. (B) Corresponding Q-$t^{1/2}$ plots.

3.3. Analytical performance

3.3.1. Calibration curve and detection limit

Under the optimal experimental conditions, DPV was used to investigate the relationship between the peak current and the concentration of CA (Fig. 10A). As shown in Fig. 10B, the peak

currents linearly increased as the concentration of CA increased within the range of 0.05 μM to 20 μM, and the linear regression equation could be expressed as I_{pa} (μA) = 4.165 C (μM) + 1.305 (R^2 = 0.9983) with a sensitivity of 27.58 μA·μM^{-1}·cm^{-2} and a detection limit of 8 nM (S/N = 3). As shown in Table 1, our ERGO-COOH/GCE had a relatively excellent detection performance compared with previously reported CA sensors.

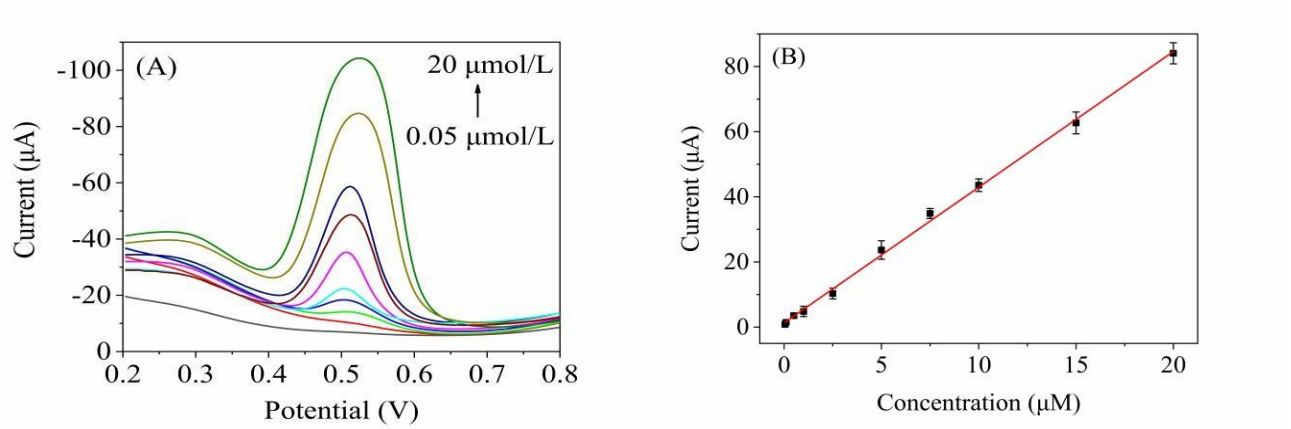

Figure 10. (A) DPV curves of CA on the ERGO-COOH/GCE in 0.04 M B-R buffer solution (pH = 2.0) at different concentrations (0.05, 0.1, 0.5, 1, 2.5, 5, 7.5, 10, 15, 20 μM) at a scan rate of 0.05 V·s^{-1}. (B) Calibration curves corresponding to the redox peak current (I_{pa}) and the concentration of CA.

Table 1. Comparison of the electrochemical sensing performance of different modified electrodes toward CA detection

Electrode	Linear range (μM)	LOD (nM)	Method	Real sample	Reference
FLD/MWCNT/SPE	2.0~50	200	DPV	Mate tea, fennel tea, white tea	[38]
CNF/C-SPE	0.1～40	3.23	CV	Active Detox, DVR-Sten Glycemo, green tea	[39]
CF-UME	1.0～500	410	CV	White wine, rose wine, red wine	[40]
f-MWCNTs/α-$NaFeO_2$/GCE	0.1～154.7	2	DPV	Coffee, green tea, red wine	[41]
SnO_2-RGO/GCE	0.15～25	80	DPV	Red wine	[42]
GR/CuO@Cu-BTC/GCE	0.02～10	7	DPV	Red wine	[43]
PEDOT-modified electrode	0.15～4	110	DPV	-	[44]
PtCu/GCE	1.2～1930	350	DPV	-	[13]
Chit-CB/rGO/GCE	0.6~106 0.0006～573	21 0.03	DPV AMP	Red wine, white wine, pink wine	[45]
CPE/MWCNTs- Bi/CTAB	0.06～500	0.157	DPV	Coconut water, coffee, tea	[46]
Cu_2S NDs@GOS NC/SPCE	0.055～2455.1	0.22	AMP	Soft drink, red wine	[47]
F-GO/GCE	0.5～100.0	180	DPV	Red wine	[18]
N-CQD@HP-Cu_2O/MWCNT/GCE	0.05～43	4	DPV	Red wine	[31]
Pt-PEDOT/rGO/GCE	0.005～50	2	DPV	Green tea, black tea	[19]
$CoFeSe_2$/f-CNF/GCE	0.01～263.96	2	DPV	Red wine	[48]
PtAuRu/GCE	8.7～16600	390	DPV	-	[49]
HMGO/GCE	0.01～608	4	AMP	Red wine	[50]
ERGO-COOH/GCE	0.05～20	8	DPV	CA tablet	This work

3.3.2. Repeatability and reproducibility of the ERGO-COOH/GCE

The repeatability and reproducibility of the ERGO-COOH/GCE were investigated by detecting the oxidation peak current of 5 μM CA by DPV. The relative standard deviation (RSD) of the oxidation peak current with fifteen consecutive measurements of CA on one ERGO-COOH/GCE was 0.8%, indicating the good repeatability of the present method (Fig. 11A). The RSD of the peak current response of CA was 2.4% with six parallel modified electrodes, proving the good reproducibility of the electrode preparation (Fig. 11B).

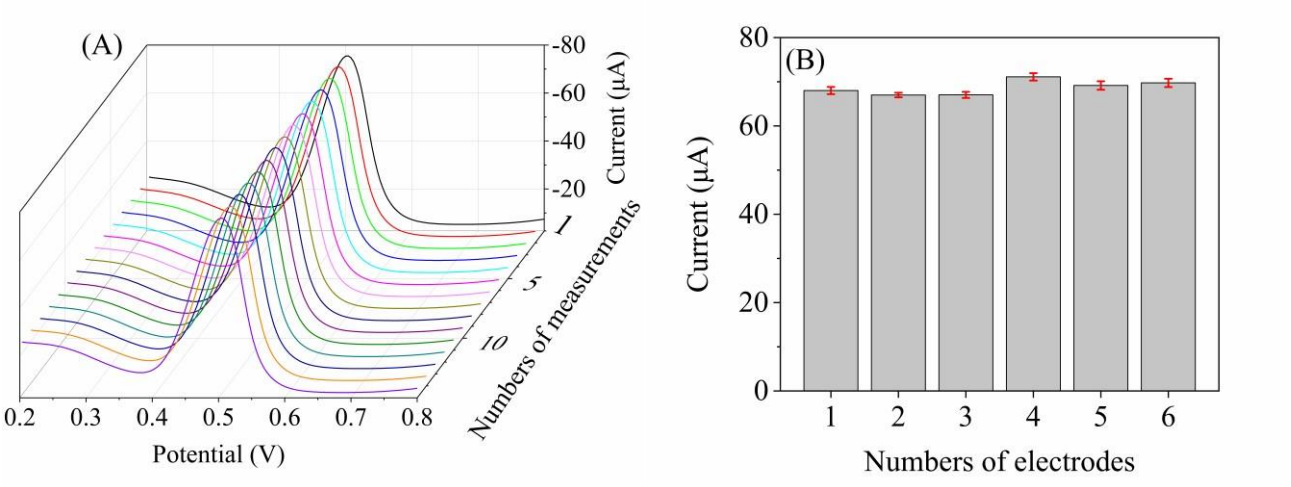

Figure 11. (A) DPV curves of 5 μM CA on the ERGO-COOH/GCE for 15 consecutive measurements. (B) DPV responses of 5 μM CA on six different ERGO-COOH/GCEs.

3.3.3. Interference studies

Under optimal experimental conditions, the possible interference from metal ions and organic compounds that may be present in pharmaceutical samples was evaluated in a 5 μM CA solution by DPV. The maximum concentration of the interfering species that caused an error of less than ±5% was defined as the tolerance limit. Fig. 12A shows that Fe^{2+}, Ca^{2+}, and CO_3^{2-} in 50-fold, Zn^{2+}, Cu^{2+}, glucose, tartaric acid, sucrose, and dextrin in 100-fold, citric acid and ascorbic acid in 150-fold, K^+, Cl^-, Na^+, Mg^{2+}, SO_4^{2-} and malic acid in 200-fold concentration of 5 μM CA did not interfere with the determination of CA. The results suggested that the ERGO-COOH/GCE had good anti-interference performance for the determination of CA.

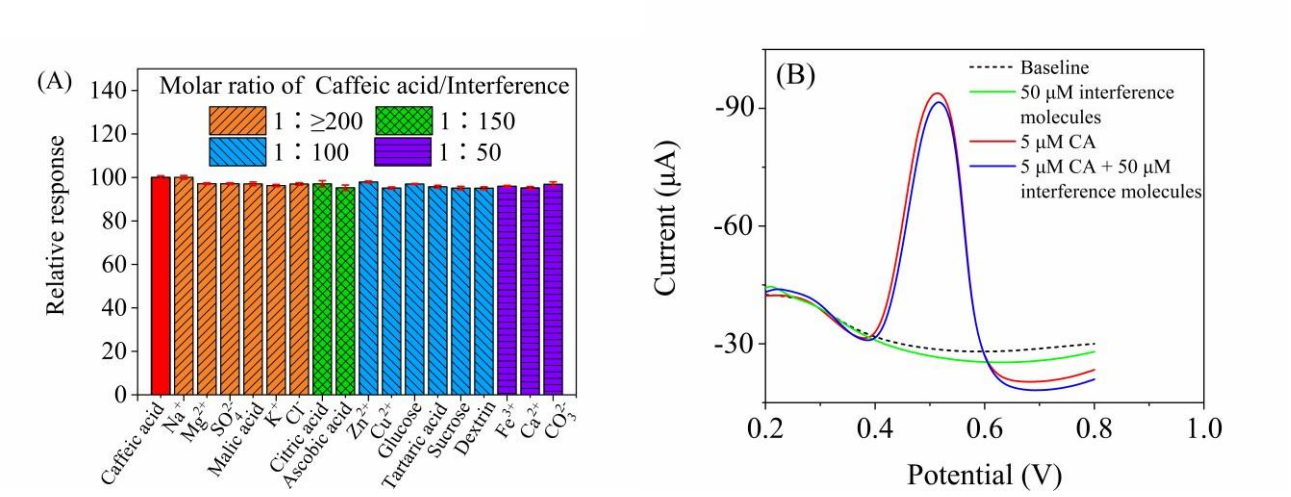

Figure 12. (A) Relative DPV response ($I_{Interference}/I_{CA}$) of 5 μM CA on the ERGO-COOH/GCE coexisting with different interferences in 0.04 M B-R (pH 2.0). (B) DPV curves of 5 μM CA with or without the presence of 50 μM malic acid, citric acid, ascorbic acid, glucose, tartaric acid, sucrose, and dextrin on ERGO-COOH/GCE.

3.4. Real sample analysis

The proposed electrochemical sensor was applied to detect CA in caffeic acid tablets to evaluate the applicability of the present method. Under optimal experimental conditions, the standard addition method was used to determine the content of CA by DPV. As shown in Table 2, the average recovery of CA on the ERGO-COOH/GCE was 104% with RSD of 5.1%, and the percentage of the labelled amount of CA in caffeic acid tablets was calculated to be 99%, which indicated that the method had excellent accuracy.

Table 2. Determination for CA in Caffeic acid tablets

Sample	Initial (μM)	Added (μM)	Found (μM)	Reference (%)	RSD (%, n=3)
Caffeic acid tablets	1.98	2.00	4.10	108	4.2
		4.00	6.14	105	3.1
		6.00	7.80	97.7	3.7

4. CONCLUSIONS

In this paper, a sensitive sensor named ERGO-COOH/GCE for the electrochemical detection of CA was developed based on GO-COOH by the electrodeposition method. The electrochemical behavior of CA was studied, and an electrochemical analysis method for the accurate detection of CA was established. Under optimal conditions, the ERGO-COOH/GCE has a high sensitivity, good precision, a

strong anti-interference ability, and a low detection limit. The prepared ERGO-COOH/GCE may be suitable for the accurate determination of CA in other drug samples and food samples.

References

1. S. A. Heleno, A. Martins, M. J. R. P. Queiroz, I. C. F. R., I. C. F. R. Ferreira, *Food Chem*., 173 (2015) 501-513.
2. C. Magnani, V. L. B. Isaac, M. A. Correa, H. R. N. Salgado, *Anal. Methods*, 6 (2014) 3203-3210.
3. H. G. Choi, P. T. Tran, J. H. Lee, B. S. Min, J. A. Kim, *Arch. Pharm. Res*., 41 (2017) 64-70.
4. Z. M. Wu, Z. J. Yu, Z. Q. Cui, L. Y. Peng, H. R. Li, C. L. Zhang, H. Q. Shen, P. F. Yi, B. D. Fu, *Microb. Pathogenesis*, 11 (2017) 240-244.
5. G. Wang, Z. Lei, Q. Zhong, W. Wu, H. Zhang, T. Min, H. Wu, F. Lai, *Food Chem*., 217 (2017) 332341.
6. L. Zhang, W. P. Zhang, K. D. Chen, X. D. Qian, S. H. Fang, E. Q. Wei, *Life Sci*., 80 (2007) 80 530537.
7. S. Y. Chiou, J. M. Sung, P. W. Huang, S. D. Lin, *J. Med. Food*, 20 (2017) 171-179.
8. V. P. Sonar, A. Corona, S. Distinto, E. Maccioni, R. Meleddu, B. Fois, C. Floris, N. V. Malpure, S. Alcaro, E. Tramontano, F. Cottiglia, *Eur. J. Med. Chem*., 130 (2017) 248-260.
9. M. Ogawa, Y. Shirasago, S. Ando, M. Shimojima, M. Saijo, M. Fukasawa, *J. Infect. Chemother*., 24 (2018) 597-601.
10. J. Wang, Y. Zhao, M. Zhang, Q. Shi, *J. Chromatogr. Sci*., 53 (2015) 526-530.
11. X. Yao, G. Chen, *Anal. Bioanal. Chem*., 388 (2007) 475-481.
12. C. Tang, O. S. Sojinu, *Talanta*, 94 (2012) 232-239.
13. Y. Shi, H. Xu, Z. Gu, C. Wang, Y. Du, *Colloid. Surface*. A, 567 (2019) 27-31.
14. B. Z. Liu, Y. R. Ma, F. Zhou, Q. Wang, G. Q. Liu, *Int. J. Electrochem. Sci*., 15 (2020) 9590-9596.
15. Q. He, Y. Wu, Y. Tian, G. Li, J. Liu, P. Deng, D. Chen, *Nanomaterials*, 9 (2019) 115.
16. C. Zhang, J. J. Ren, Y. F. Xing, M. Cui, N. Li, P. Liu, X. F. Wen, M. Li, *Mat. Sci. Eng. C.*, 108 (2020) 110214.
17. N. Karikalan, R. Karthik, S. M. Chen, H. A. Chen, *Sci. Rep*., 7 (2017) 45924.
18. V. S. Manikandan, B. Sidhureddy, A. R. Thiruppathi, A. Chen, *Sensors*, 19 (2019) 1604.
19. L. Gao, R. Yue, J. Xu, Z. Liu, J. Chai, *J. Electroana. Chem*., 816, (2018) 14-20.
20. K. Tyszczuk, A. Skalska-Kamińska, A. Woźniak, *Food Chem*., 125 (2011) 1498-1503.
21. Q. Tang, Z. Zhou, Z. Chen, *Nanoscale*, 5 (2013) 4541-5130.
22. Z. U. Khan, A. Kausar, H. Ullah, *Polym. Plast. Technol. Eng*., 55 (2015) 559-581.
23. M. Zhou, Y. J. Sheng, Y. C. Li, R. Y. Wang, *Int. J. Electrochem. Sci*., 16 (2021) 210438.
24. X. Ma, Y. Wu, S. Devaramani, C. Zhang, Q. Niu, M. Ibrahim-Shinger, W. Li, D. Shan, X. Lu, *Talanta*, 178 (2018) 962-969.
25. Y. Dilmac, M. Guler, *J. Electroanal. Chem*., 864 (2020) 114091.
26. M. Song, J. Xu, *Electroanal*., 25 (2013) 523-530.
27. Y. W. Xu, W. Zhang, J. Y. Shi, X. B. Zou, Y. X. Li, E. T. Haroon Elrasheid, X. W. Huang, Z. H. Li, X. D. Zhai, X. T. Hu, *Food Chem*., 237 (2017) 423-430.
28. C. Karuppiah, S. Cheemalapati, S. M. Chen, S. Palanisamy, *Ionics*, 21 (2014) 231-238.
29. W. Sun, Y. Zhang, X. Ju, G. Li, H. Gao, Z. Sun, *Anal. Chim. Acta*, 752 (2012) 39-44.
30. A. P. Fan, L. Shi, H. P. Yang, G. M. Yang, *Int. J. Electrochem. Sci*., 15 (2020) 9669-9682.
31. G. Muthusankar, M. Sethupathi, S. M. Chen, R. K. Devi, R. Vinoth, G. Gopu, N. Anandhan, N. Sengottuvelan, *Compos. Part* B, 174 (2019) 106973.
32. I. Karaduman, E. Er, H. Çelikkan, N. Erk, S. Acar, *J. Alloy. Compd*., 722 (2017) 569-578.
33. H. Filik, G. Çetintaş, A. A. Avan, S. Aydar, S. N. Koç, İ. Boz, *Talanta*, 116 (2013) 245-250.

34. J. Ning, Q. He, X. Luo, M. Wang, D. Liu, J. Wang, J. Liu, G. Li, *Sensors*, 18 (2018) 2762.
35. M. Arvand, A. Shabani, M. S. Ardaki, *Food Anal. Method*., 10 (2017) 2332-2345.
36. E. Laviron. *J. Electroanal. Chem*., 101 (1979) 19-28.
37. F. C. Anson, *Anal. Chem*., 36 (1964) 932-934.
38. D. A. G. Araujo, J. R. Camargo, L. A. Pradela-Filho, A. P. Lima, R. A. A. Munoz, R.M. Takeuchi, B.C. Janegitz, A. L. Santos, *Microchem. J*., 158 (2020) 105297.
39. A. V. Bounegru, C. Apetrei, *Chemosensors*, 8 (2020) 41.
40. A. Gevaerd, B. M. da Silva, P. R. de Oliveira, L. H. Marcolino Júnior, M. F. Bergamini, *Anal. Methods*, 12 (2020) 3608-3616.
41. R. Nehru, Y. F. Hsu, S. F. Wang, *Anal. Chim. Acta*, 1122 (2020) 76-88.
42. J. W. Zhang, K. P. Wang, X. Zhang, *Mater. Res. Bull*., 126 (2020) 110820.
43. X. Tu, Y. Xie, F. Gao, X. Ma, X. Lin, X. Huang, F. Qu, L. Ping, Y. Yu, L. Lu, *Microchim. Acta*, 187 (2020) 258.
44. V. Karabozhikova, V. Tsakova, *Electrochim. Acta*, 293 (2019) 439-446.
45. K. Pandian, D. M. Soundari, P. R. Showdri, J. Kalaiyarasi, S. C. B. Gopinath, *Microchim. Acta*, 186 (2019) 54.
46. V. Erady, V. Erady, R. J. Mascarenhas, A. K. Satpati, A. K. Bhakta, Z. Mekhalif, J. Delhalle, D. A, *Microchem. J*., 146 (2019) 73-82.
47. T. W. Chen, U. Rajaji, S. M. Chen, M. Govindasamy, S. S. P. Selvin, S. Manavalan, R. Arumugam, *Compos. Part* B, 158 (2019) 419-427.
48. M. Sakthivel, S. Ramaraj, S. M. Chen, B. Dinesh, H. V. Ramasamy, Y. S. Lee, *Anal. Chim. Acta*, 1006 (2018) 22-32.
49. Y. Shi, H. Xu, J. Wang, S. Li, Z. Xiong, B. Yan, C. Wang, Y. Du, *Sensor. Actuat. B: Chem*., 272 (2018) 135-138.
50. K. Sivasankar, R. Devasenathipathy, S. F. Wang, K. Kohila rani, D. S. Raja, C. H. Lin, *J. Taiwan Inst. Chem. E*., 84 (2018) 188-195.